JOURNAL OF MATERIALS SCIENCE **34** (1999) 3525–3531

Carbide surface coating of Co-Cr-Mo implant alloys by a microwave plasma-assisted reaction

N. S. VANDAMME, L. QUE, L. D. T. TOPOLESKI
Department of Mechanical Engineering, UMBC, Baltimore, MD 21250, USA

A technique to grow a hard carbide surface coating on Co-Cr-Mo implant alloys used in artificial joints was developed. The carbide surface coating was applied to as-cast and forged Co-Cr-Mo alloys to improve their wear properties. The surface carbide layers were produced by reactions between the alloy surface and a methane-hydrogen mixed gas by a microwave plasma-assisted surface reaction. The new carbide layers showed "brain coral-like" surface morphology and appear to consist of mixed phases including Cr_3C_2, Cr_2C, Cr_7C_3, $Cr_{23}C_6$, and Co_2C. The Vickers microhardness of thin carbide coatings ($\sim$3 μm thick) was about HV 1100 regardless of the test location. The Vickers microhardness of thick carbide coatings ($\sim$10 μm thick) showed a wide range of hardnesses from HV 1000 to HV 2100. Co-deposition of soot and diamond films occured on a small area of the forged alloy substrates and diamond particles were sparsely dispersed on as-cast alloy substrates. The carbide surface layer has the potential to increase the wear resistance of the Co-Cr-Mo alloy as a wear resistant coating.

1. Introduction

There is a growing concern about the wear of materials used in artificial joints. Ultrahigh molecular weight polyethylene (UHMWPE) and metal wear debris have been linked to component loosening and osteolysis [1–3]. The wear mechanisms of metal artificial joint components are critical to understanding the failure of artificial joint materials and improving their performance. For example, acrylic bone cement particles and bone debris introduced into metal/UHMWPE wear couples cause wear of the metal [4–6]. Increased metal surface roughness may subsequently lead to accelerated UHMWPE wear [7, 8].

Surface modification is one important approach to improving wear resistance as well as developing new materials. For example, amorphous diamond-like carbon coatings and ion implantation have been used to improve the wear resistance of 316 stainless steel, Co-Cr, and Ti-6Al-4V alloys [6, 9–13]. Coatings of chromium carbides, such as Cr_3C_2 and Cr_7C_3, have been produced by the laser cladding [14, 15] and the plasma spray methods [16] and studied as candidates for hardfacing coatings in high temperature applications due to their excellent abrasive wear resistance and corrosive resistance.

This paper reports on the formation of metal carbide surface layers on a Co-Cr-Mo alloy by the reaction between the alloy surface and gases by a microwave plasma-assisted surface reaction. The carbide surface has the potential to improve the wear performance of Co-Cr-Mo alloy joints.

2. Experimental

Pieces of as-cast (F75) and forged (F799) Co-Cr-Mo alloys were cut into 10 mm $\times$ 10 mm $\times$ 3 mm specimens. The manufacturer's certifications gave the primary composition of the alloy as 64-wt % Co, 28-wt % Cr, and 5-wt % Mo. The carbon content of the as-cast and forged alloys were 0.25 and 0.054 wt %, respectively. Prior to plasma processing, the top surfaces of the specimens were polished with #800 SiC abrasive paper and then 3-μm diamond suspension to a "mirror finish" and ultrasonically cleaned with acetone. The average roughness (Ra) was 0.01 μm, measured with a profilometer (NewView 100, Zygo, Inc., Conn.).

A microwave plasma-assisted chemical vapor deposition (MPCVD) system originally designed for diamond film deposition was used to create the carbide layers. The system is equipped with a tubular fused quartz reaction chamber with a 34 mm inner diameter similar to that of Kamo *et al*. [17]. The microwave generator (Toshiba Corp.) provides from 0.1 to 1.5 kW of microwave power at a frequency of 2.45 GHz. The Co-Cr-Mo specimens were mounted on a graphite holder and inserted into a confined plasma space on a fused quartz rod. Plasma processing was carried out in a mixture of methane (Ultra High Purity 99.97%) and hydrogen (Zerograde 99.99%) with a total gas pressure of 70 Torr and a total gas flow rate of 100 sccm (1 sccm of CH_4 and 99 sccm of H_2) for 5–10 h. Before introducing methane, the substrates were immersed in hydrogen plasma for 15 minutes. The substrate temperature was controlled by changing the microwave input

power. The substrate temperature was maintained at 1000 ± 50 °C which was measured with an optical pyrometer (Leeds and Northrup Model 8622) through the quartz-glass viewport at the top of the reaction chamber. As-cast and forged Co-Cr-Mo substrates were treated side-by-side in the plasma processing chamber.

Coated surfaces were characterized by X-ray diffraction (XRD) analysis using a CuK_α source with Ni filter (Philips PW1729 X-ray generator and a multichannel analyzer Canberra S100 with a Ge solid state detector), scanning electron microscope (SEM) (JEOL JSM-35CF) observation, surface profilometry with the Zygo-NewView 100 profilometer, and hardness tests with a microhardness tester (MICROMET 1, Buehler Ltd.). The preliminary wear property study of the carbide coated Co-Cr-Mo was carried out using a four-station-wear-test fixture and the torsional mode on an MTS 858 Bionix biaxial testing system.

3. Results and discussion

Silver colored surface layers were formed on both types of Co-Cr-Mo substrates, and dark gray deposits covered a small part of the forged alloy substrates (Fig. 1). The dark gray area consisted of a powdery black bottom layer and fragile dark gray top film. The coating produced in a 6-h processing time on as-cast Co-Cr-Mo substrate consisted of a dense bottom layer and a top layer with a unique surface morphology (Fig. 2). Linearly and circularly linked crystalline grain clusters were randomly arranged and made up uniformly distributed convolutions similar to "brain coral". The grain size in the dense bottom layer was about 1 μm. The size of crystalline grains in the top cluster layer was 3–4 μm. The height of the top cluster layer was 2–3 μm as measured with the profilometer. The total thickness of the surface coating was about 10 μm estimated from the SEM photo of a polished section of the side plane of the substrate.

The coating produced in a 6-h processing time on forged Co-Cr-Mo substrate was different (Fig. 3). Three distinctly different deposits can be observed. The silver colored area showed a coating similar to that on the as-cast Co-Cr-Mo substrate except for discrete island-like crystalline grain clusters in the top layer. The fragile dark gray top film was a diamond film which consisted of loosely connected diamond crystals with their characteristic twinned and defective crystals [18]. The film was sitting on a fine powdery layer of soot.

The transition metal elements Co and Cr, which are the main components of the studied alloys, are known to form a wide variety of carbides [19]. Among known carbides, Cr_7C_3-type and $Cr_{23}C_6$-type carbides are found to be internal precipitates and contribute to the mechanical properties of the Co-Cr-Mo alloy [20–23]. The XRD patterns of the silver colored coating on the as-cast Co-Cr-Mo substrate are shown in Fig. 4. Possible peak assignments include those for hexagonal Cr_7C_3, orthorhombic Cr_7C_3, hexagonal Cr_2C, cubic $Cr_{23}C_6$, orthorhombic Cr_3C_2, and Co_2C [24]. While many diffraction peak positions of the coated substrate agree with those of hexagonal Cr_7C_3, the diffraction angle of the strongest peak in our specimens ($2\theta = 43.0°$) agrees with the strongest peaks of hexagonal Cr_2C and Co_2C carbides. The lattice parameters calculated from the assigned peaks are: $a = 1.400 \pm 0.003$ nm and $c = 0.448 \pm 0.003$ nm for hexagonal Cr_7C_3, $a = 0.279 \pm 0.002$ nm and $c = 0.435 \pm 0.01$ nm for hexagonal Cr_2C, and $a = 1.066 \pm 0.002$ nm for cubic $Cr_{23}C_6$ carbides. These values are in good agreement with those reported in the ASTM XRD files: $a = 1.398$ and $c = 0.452$ nm for hexagonal Cr_7C_3, $a = 0.279$ and $c = 0.446$ nm for hexagonal Cr_2C, and $a = 1.066$ nm for cubic $Cr_{23}C_6$ carbides [24]. Unidentified peaks were observed, however, and some strong peaks for the carbides were absent in our specimens. Although the microwave plasma environment is likely to induce metastable phases and to form hydrides because the plasma contains active atomic and molecular species of hydrogen and hydrocarbon, the surface coating produced on Co-Cr-Mo alloy seemed to consist of mixed phases including Cr_3C_2, Cr_2C, Cr_7C_3, $Cr_{23}C_6$, and Co_2C. The metal carbides may actually have a ternary solid solution composition such as, M_7C_3 for example,

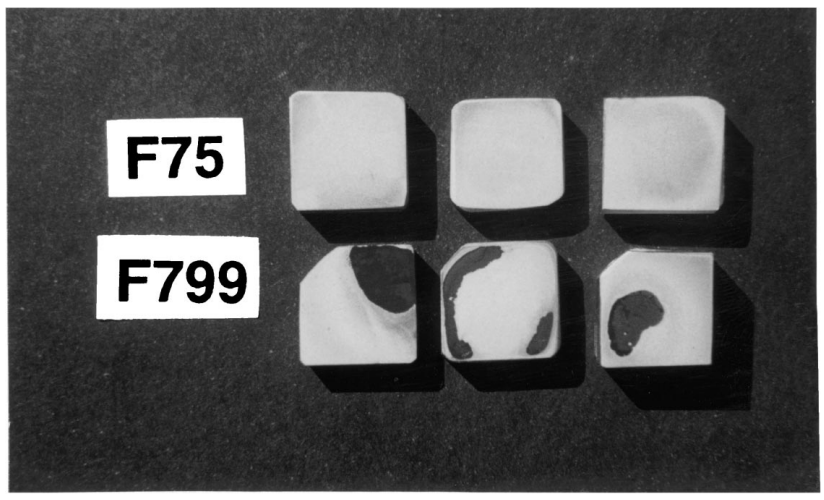

Figure 1 Examples of 6-h plasma processed Co-Cr-Mo substrates (about 10 mm × 10 mm × 3 mm). A pair of (top) as-cast (F75) and forged (F799) (bottom) specimens was treated together side-by-side.

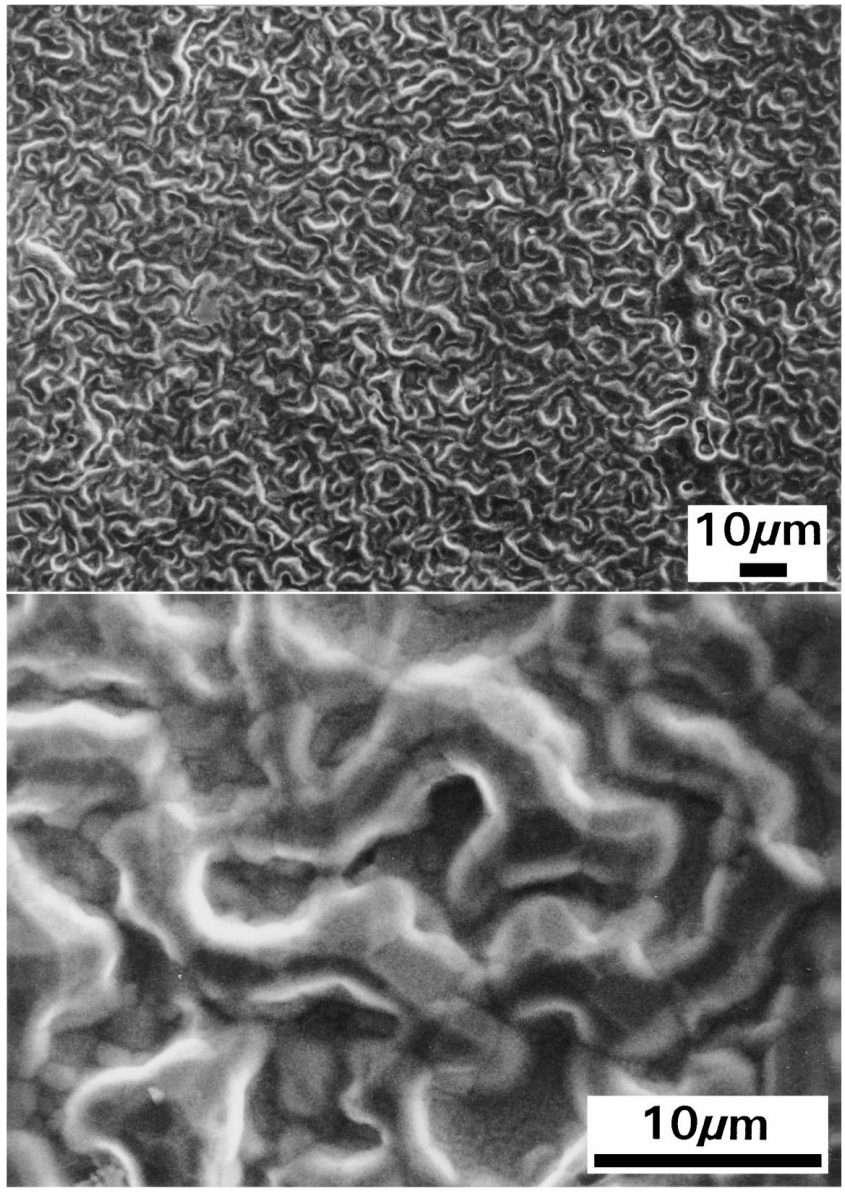

Figure 2 SEM photos of a coating with 6-h processing time on as-cast Co-Cr-Mo substrate.

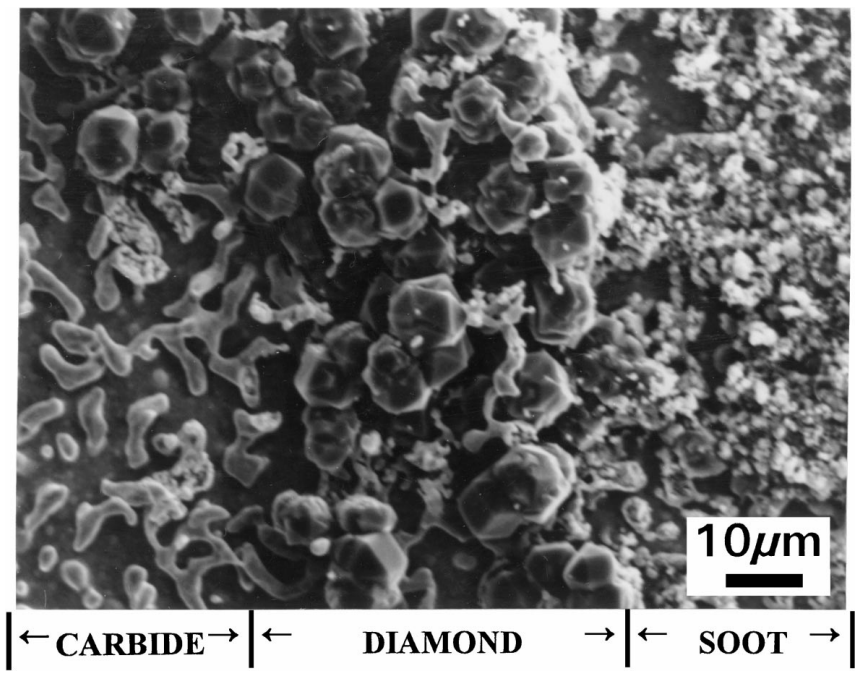

Figure 3 SEM photo of a coating with 6-h processing time on forged Co-Cr-Mo substrate. The location near the dark gray area shown in Fig. 1 is field of focus. A diamond film can be seen in the center. A layer of soot on the right side was exposed by removing a part of the diamond film.

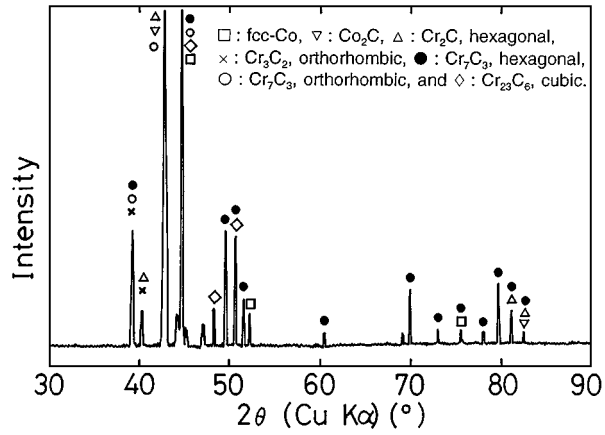

Figure 4 XRD pattern of the silver colored coating on as-cast Co-Cr-Mo substrate.

where $M =$ Co, Cr, and Mo. The relationship between the "brain coral-like" morphology, the crystal structure of metal carbides, and the surface grain boundary structure of the base alloys may control the growth mechanism of surface carbides on Co-Cr-Mo alloys. More extensive study is necessary to determine the phase, composition, and growth mechanism of surface carbides.

In our present system, carbon is supplied continuously, while the source of metal is the substrate. Carbon atoms produced from the decomposition of methane diffuse into the Co-Cr-Mo alloy substrates in the initial stage of plasma processing, similar to the conventional carburization of steel. After the carbon content in the alloy matrix reaches the saturation level of solid solution or precipitates, the formation of surface carbide layers may start. The weight in the Co-Cr-Mo specimens increased with an increase in plasma processing time (Fig. 5). After the initial weight measurement at 25 min of plasma processing, the weight of the Co-Cr-Mo specimens was measured after every two hours of plasma processing. Non-linear regression analysis showed that the as-cast and forged alloy substrate weight gain followed the equations $\Delta W = (9.5t)^{1/2.0}$ and $\Delta W = (52.6t)^{1/2.3}$, respectively, where t is processing time in hours and ΔW is weight gain in mg/cm^2. The parabolic relationship is commonly observed between

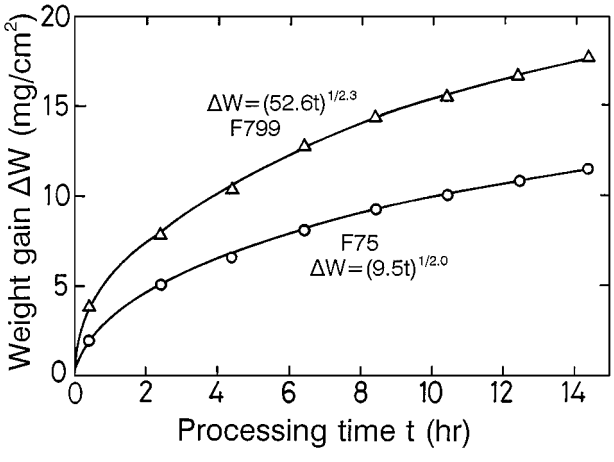

Figure 5 Weight gain in Co-Cr-Mo alloy substrates with an increase in processing time.

TABLE I Vickers microhardness of as-cast and forged Co-Cr-Mo alloy substrates with and without carbide surface coatings

	As-cast (F75)	Forged (F799)
Carbide surface coatings	Thin coatings 1100 ± 80 Thick coatings 1000–2100	
Surface after carbide layer polished away	880 ± 60	860 ± 60
1.5 mm below surface	340 ± 30	390 ± 30
Original alloy matrix	350 ± 20	430 ± 20

weight gain and time in conventional steel carburization, where the kinetics of the carburization reaction are controlled by carbon diffusion processes [25–27]. The forged alloy showed more weight gain than the as-cast alloy. Since the initial carbon content of the forged alloy is about one fifth of that in the as-cast alloy, a greater part of the weight gain in the forged alloy is likely due to the carbon atom diffusion into the alloy bulk. As the formation of the carbide surface layers proceeds, the growth of metal carbides is ultimately controlled by metal atom diffusion from the surface through carbide layers. The ultimate coating thickness, therefore, is likely to be limited by metal atom diffusion in the carbide layers.

A wide range of hardness, 1000–2900 Vickers microhardness, has been reported for chromium carbides [14, 28, 29]. The results of Vickers microhardness measurements with test loads of 50, 100, and 200 gf of our specimens are shown in Table I, where each hardness value is the average of six to twelve measured points using two specimens for each material. The hardnesses of the original alloy matrix of as-cast (F75) and forged (F799) alloy substrates are HV 350 ± 20 and HV 430 ± 20, respectively. While the hardness of the thin carbide coatings ($\sim$3 μm thick) was about HV 1100 regardless of the test location, the thick carbide coatings ($\sim$10 μm thick) showed a wide range of hardness from HV 1000 to HV 2100. This wide range of hardness can be attributed to the mixed phases and unique surface morphology of the coating.

The hardness depth profile was measured on a polished cross section of the carbide coated substrate which was cut along its center perpendicular to the carbide surface layers. The hardness of the carbide coated as-cast substrate at about 50 μm below the original surface was about HV 850. This value is very close to the HV 880 hardness of its surface after the carbide layers were polished away. The hardness decreased rapidly down to HV 500 at 200 μm below the surface. At 1.5 mm below the surface, the hardness was about HV 340 and almost equal to that of the alloy matrix before plasma processing. The result of the depth profile shows that a hardened layer of about 100 μm was formed by carbon diffusion under the hard carbide surface layers.

Indenting the carbide coated specimens with a Rockwell hardness diamond cone under a 150 kg load produced microcracks only 3 to 5 μm long in the 30 μm-wide area adjacent to the circular indentation mark along the circumferential direction (Fig. 6). There

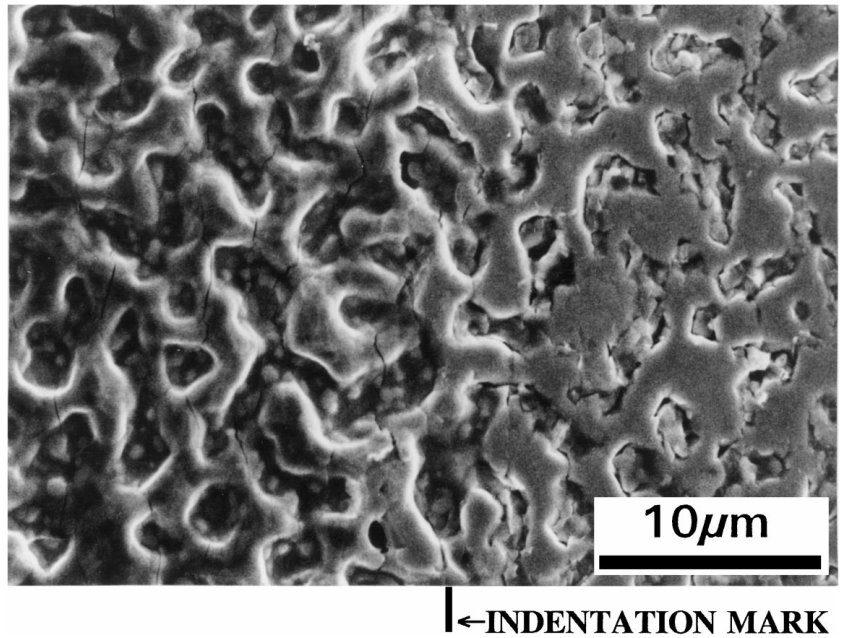

Figure 6 SEM photo of the adjacent area of the circular indentation mark made by Rockwell hardness tester diamond cone under a 150 kg load on a carbide coated Co-Cr-Mo substrate. The right half is inside the indentation mark.

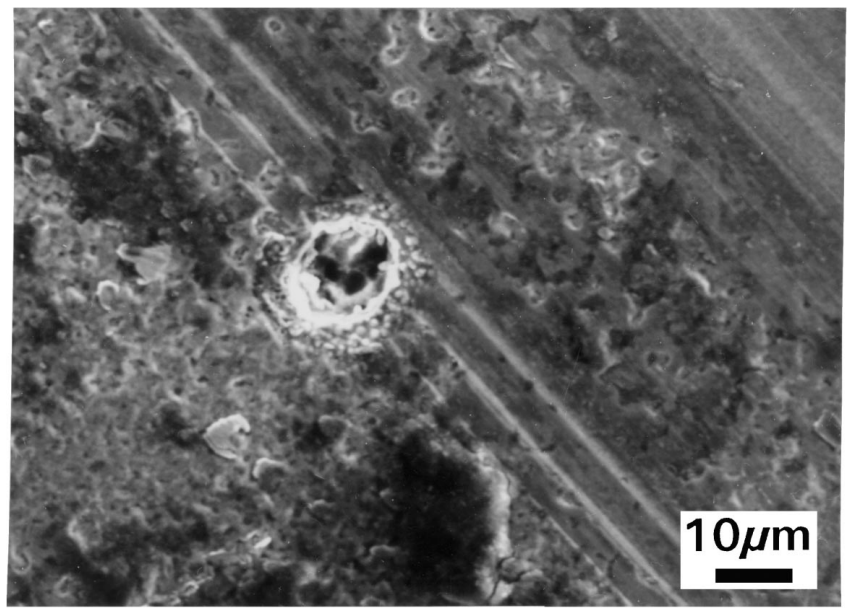

Figure 7 SEM photo of severe scratch lines on a carbide coated Co-Cr-Mo substrate after wear test. A nest-like structure can be seen in the middle of the scratch line.

was no coating delamination. SEM photos of the indentation marks left by the Vickers microhardness diamond pyramid showed that the edges of the square indentation marks were not sharp because of broken fragments of carbide grains. No radial cracks propagating from the indentation corners were observed. The strong coating adhesion seems to arise because the carbide coating is an integral part of the substrate.

With the expectation that the "brain coral-like" surface morphology may have the advantages of retaining lubricant between the contacting solid interfaces and trapping debris which causes three-body abrasion, preliminary wear tests of carbide coated substrates were carried out against UHMWPE counterface plates in deionized water. To our surprise, the carbide coated as-cast alloy surface showed several severe scratches after a reciprocating sliding distance totaling about 6.8 km. Circular objects were observed in the middle of some severe scratch lines as shown in Fig. 7. These circular objects were found to be nest-like structures for crystalline diamond particles, and the diamond particles dislodged from the nest-like structures caused the severe scratches. Fig. 8 shows an SEM photo of untouched diamond particles grown in the nest-like structure on a carbide coated as-cast substrate. The site density of diamond particles in the nest-like structures was of the order of 10 to 100 per cm^2 depending on the carbide coated as-cast substrates. Some of the diamond particles could be removed by ultrasonic agitation in acetone, but others were strongly bonded to the substrate.

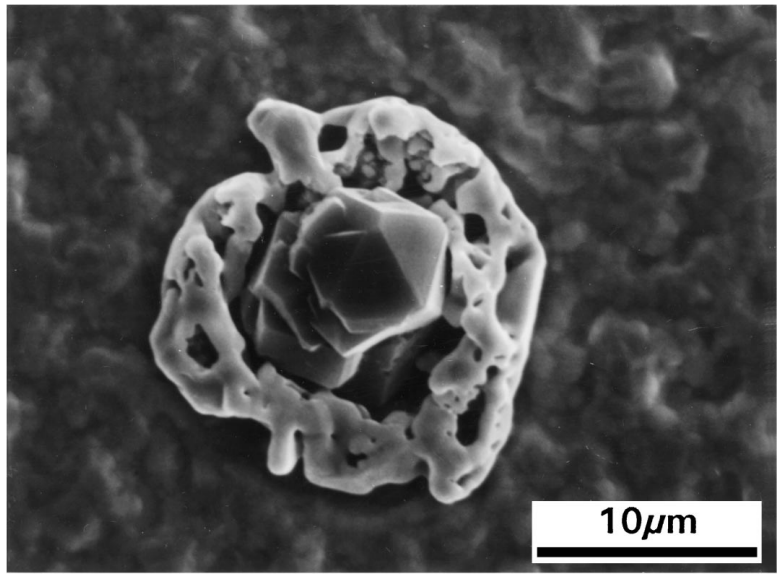

Figure 8 SEM photo of diamond particles grown in the nest-like structure on a carbide coated as-cast Co-Cr-Mo substrate.

The strongly bonded diamond particles were removed using #800 SiC abrasive paper, and wear tests were carried out against UHMWPE counterface plates and polymethylmethacrylate (PMMA) bone cement third body particles dispersed in deionized water. This time, no severe scratches were produced. The total sliding distance of about 8.3 km was not long enough to produce any significant difference in wear properties between control specimens without carbide coatings and carbide coated Co-Cr-Mo substrates. Fine scratches produced by the SiC paper used to remove the diamond particles may obscure the results of the wear test. Further wear tests with carbide surface coated Co-Cr-Mo alloy substrates free from diamond particles are necessary. Diamond particle formation may be prevented by controlling process conditions.

4. Summary

Metal carbide surface layers with an interesting surface morphology were formed on Co-Cr-Mo alloy substrates by the microwave plasma-assisted surface reaction between a mixture of methane and hydrogen and substrate materials. These carbide layers showed a wide range of hardness from HV 1000 to HV 2100 due to the mixed phases and unique surface morphology. A soot layer, and then diamond films, were formed in some places on forged (F799) substrates, but diamond particles were formed sparsely on as-cast (F75) substrates. It is necessary to prevent the formation of diamond films and particles to use carbide surface films on Co-Cr-Mo alloys to increase wear resistance.

Acknowledgements

The authors would like to thank Dr. L. Takacs for XRD analysis, Mr. P. Rutledge for SEM measurements, and Dr. O. Vesnovsky and Mr. X. Lu for their valuable support. The authors are also very grateful to Dr. R. Woods from Kirscher Inc. and Dr. R. Swain from Smith & Nephew Richards Inc. for donating alloy materials. This work was partially supported by grants from the Arthritis Foundation and the National Science Foundation.

References

1. H. A. MCKELLOP, in "Controversies of Total Knee Arthroplasty," edited by V. M. Goldberg (Raven Press, New York, 1991) p. 51.
2. H. C. AMSTUTZ, P. CAMPBELL, N. KOSSOVSKY and I. C. CLARKE, *Clinical Orthopaedics and Related Research* **276** (1992) 7.
3. D. DOWSON, *Wear* **190** (1995) 171.
4. H. MCKELLOP, I. CLARKE, K. MARKOLF and H. AMSTUTZ, *J. Biomed. Mater. Res.* **15** (1981) 619.
5. L. QUE and L. D. T. TOPOLESKI, in Trans. 21st Annual Meeting of Society for Biomaterials, 1995 p. 167.
6. H. MCKELLOP and T. V. RÖSTLUND, *J. Biomed. Mater. Res.* **24** (1990) 1413.
7. B. WEIGHTMAN and D. LIGHT, *Biomaterials* **7** (1986) 20.
8. L. QUE and L. D. T. TOPOLESKI, *J. Biomed. Mater. Res.*, accepted.
9. J. L. HAILEY, P. FIRKINS, R. BUTTER, A. H. LETTINGTON and J. FISHER, in Trans. of Fifth World Biomaterials Congress, 1996 p. 785.
10. T. L. JACOBS, J. H. SPENCE, S. S. WAGAL and H. J. OIEN, in "Applications of Diamond Films and Related Materials: Third International Conference," edited by A. Feldman, Y. Tzeng, W. A. Yarbrough, M. Yoshikawa and M. Murakawa (NIST, Gaithersburg, MD, 1995) p. 753.
11. R. S. BUTTER and A. H. LETTINGTON, *ibid.*, p. 683.
12. A. CIGADA, S. FARE, F. BROSSA, L. PARACCHINI, M. ULIVI and J. C. BRIGNOLA, in Trans. of Fifth World Biomaterials Congress, 1996 p. 789.
13. P. SHIOSHANSI and D. E. FERGUSON, *Mater. Technol.* **8** (1993) 30.
14. A. KAGAWA and Y. OHTA, *Mater. Sci. Technol.* **11** (1995) 515.
15. T. H. KIM and B. C. KIM, *J. Mater. Sci.* **27** (1992) 2967.
16. C. DELLACORTE and H. E. SLINEY, *Lubrication Engineering* **44** (1988) 338.
17. M. KAMO, Y. SATO, S. MATSUMOTO and N. SETAKA, *J. Cryst. Growth* **62** (1983) 642.
18. K. E. SPEAR, *J. Amer. Ceram. Soc.* **72** (1989) 171.
19. L. E. TOTH, "Transition Metal Carbides and Nitrides" (Academic Press, New York, 1971) p. 2.
20. L. SHI, D. O. NORTHWOOD and Z. CAO, *J. Mater. Sci.* **28** (1993) 1312.
21. R. N. J. TAYLOR and R. B. WATERHOUSE, *ibid.* **18** (1983) 3265.

22. T. KILNER, R. M. PILLIAR, G. C. WEATHERLY and C. ALLIBERT, *J. Biomed. Mater. Res.* **16** (1982) 63.
23. V. M. DESAI, C. M. RAO, T. H. KOSEL and N. F. FIORE, *Wear* **94** (1984) 89.
24. ASTM X-ray diffraction files 11-550 for hexagonal Cr_7C_3, 36-1482 for orthorhombic Cr_7C_3, 14-519 for hexagonal Cr_2C, 35-783 for cubic $Cr_{23}C_6$, 35-804 for orthorhombic Cr_3C_2, and 5-0704 for Co_2C, American Society for Testing and Materials, Philadelphia, PA.
25. ASM Committee on Gas Carburizing, "Gas Carburizing" (American Society for Metals, OH, 1964) p. 50.
26. T. A. RAMANARAYANAN and D. J. SROLOVITZ, *J. Electrochem. Soc.* **132** (1985) 2268.
27. H. M. TAMANCY and N. M. ABBAS, *J. Mater. Sci.* **27** (1992) 1061.
28. S. MOTOJIMA and S. KUZUYA, *J. Cryst. Growth* **71** (1985) 682.
29. E. K. STORMS, "The Refractory Carbides" (Academic Press, New York, 1967) p. 108.

Received 29 September 1997
and accepted 7 December 1998